# Sterile neutrinos in the early Universe

Ivashko, A.

# Chapter 1

# Introduction

## 1.1 The Standard Model of particle physics

One of the greatest achievements of theoretical physics in the XX century is the establishment of the Standard Model (SM) of elementary particles and interactions. This theory describes successfully the Universe at the smallest known scales (probed at high-energy accelerators like the Large Hadron Collider at CERN), and at the largest, cosmological scales. Historically, the electromagnetic forces (like those which bind nuclei and electrons into atoms), the weak forces (responsible for the nuclear beta-decay) and the strong forces (which form nuclei from nucleons) were thought to be disconnected in their origin. However, the attempts to build a consistent theory of weak interactions gave unphysical predictions for the scattering processes (like $e\nu \to e\nu$) at large energies. In order to change the situation, it was suggested that weak and electromagnetic interactions are unified at large energies [1, 2, 3], in a framework of $SU_L(2) \times U_Y(1)$ gauge theory. This unification predicted the existence of new particles, and in further attempts to build a complete and self-consistent theory, people were *forced* to introduce even more new particles. Since the 1960s, when the simplest version of the unified theory was first proposed, we have found many of these particles. Together with the recent discovery of the Higgs boson, *all* the predicted particles have been finally observed, and their properties match the theoretical predictions. Meanwhile, it turned out that the strong interactions are mediated by gauge forces as well [4, 5] with group $SU_C(3)$, which allowed to include the strong interactions in the framework of a single $SU_L(2) \times U_Y(1) \times SU_C(3)$ gauge theory. This theory is actually what we call the Standard Model.

It is worth noting here that the SM has a peculiar structure. First, there is the intrinsic violation of parity under spatial reflections ($P$-violation). In particular, neutrinos can be only left-handed, and although the other fermions have both left and right components, these left and right components act differently in electroweak interactions (for example, right components do not take part in $SU_L(2)$ interaction). Second, the fermions are organized in three copies (generations), which have identical properties, except for the mass. Among the other peculiarities are the very small magnitude of $CP$-violation and the wide range of the masses of fermions (they span many orders of magnitude).

## 1.2 Beyond the Standard Model (BSM) phenomena

Despite the great success of the SM, which has been confirmed in numerous accelerator experiments, in the process of testing this model a number of *observable* phenomena in particle physics, astrophysics, and cosmology were found that remain unexplained. These problems, which usually are referred to as the *Beyond the Standard Model* (BSM) problems, indicate that the SM is not the final theory. It is worth noting that the BSM problems were found initially in the *non-accelerator observations*, as we will see below.

### 1.2.1 Neutrino masses and oscillations

The first BSM problem that we will consider is the existence of **neutrino oscillations**. In the Standard Model, there are three types (flavours) of neutrinos: electronic ($\nu_e$), muonic ($\nu_\mu$), and tauonic ($\nu_\tau$). **Neutrino oscillations are the transitions of one neutrino flavour into another, which take place even in empty space (in vacuum).**

The existence of these transitions indicates that the numbers of particles of a given flavour (lepton numbers) are not conserved individually. The indication for neutrino oscillations was first found in studies of fluxes of solar neutrinos [6], which were different from the theoretical expectations based on the so-called Standard Solar Model. The experimental evidence in favour of oscillations has grown: oscillations were confirmed for neutrinos that come from interactions of high-energy particles with the Earth atmosphere [7], reactor neutrinos [8, 9, 10] and accelerator neutrinos [11, 12, 13] oscillate as well. The results of all the well-established experiments in the domain of oscillations fit into the three-flavour mixing scheme [14], for a review, see [15]. In this scheme, neutrinos have mass, but a state with definite flavour does not have a definite mass. In other words, the basis of quantum-mechanical *mass* eigenstates does not coincide with the basis of *flavour* eigenstates, but these two bases are related by a non-trivial linear transformation described by unitary matrix, which is called the Pontecorvo-Maki-Nakagawa-Sakata matrix [16, 17, 18].

It is interesting to note that neutrino oscillations *can* be included in the Standard Model. Indeed, oscillations can be described by including the Majorana mass terms $m_{\alpha\beta}\overline{\nu_\alpha^c}\nu_\beta$ in the Lagrangian. However these terms do not obey $SU_L(2)$

gauge invariance of the theory, since the neutrino field $\nu_\alpha$ ($\alpha = e, \mu, \tau$) is a component of the $SU_L(2)$ lepton doublet $L$ ($L_e = (\nu_e, e)^T$), which mixes with the other component under the gauge transformation. In order to write a gauge-invariant Lagrangian, which describes neutrino masses, one has to introduce the Higgs doublet field $H$,

$$\Delta\mathcal{L} = \sum_{\alpha,\beta} \frac{F_{\alpha\beta}}{\Lambda} (\overline{L_\alpha}\tilde{H})(H^\dagger L^c_\beta), \tag{1.1}$$

As a result, we get a higher-order operator, the so-called Weinberg operator [19]. Here $L^c = i\gamma^2(L^\dagger_\alpha)^T$ is the charge-conjugated leptonic field, $\tilde{H} = i\sigma_2(H^\dagger)^T$. Then, after the spontaneous breaking of electroweak symmetry, neutrinos receive masses of order $Fv^2/\Lambda$, where $v \sim 200\,\mathrm{GeV}$ is the vacuum expectation value of the Higgs field, and $F$ is a typical value of the matrix elements $F_{\alpha\beta}$. By a rescaling of variables $F$ and $\Lambda$, one can make $F \sim 1$ without loss of generality. Noting that the cosmological and terrestial observations imply an upper bound on the neutrino masses of order of eV [20, 21], we conclude that $\Lambda \gtrsim 10^{14}\,\mathrm{GeV}$. Although the Standard Model can accomodate the neutrino oscillations by introducing the Weinberg operator, this higher-order correction implies existence of new physics (which is not captured by the Standard Model) at the energy $E$ which cannot be higher than $\Lambda$.[1] At the same time, although the energy scale of $10^{14}\,\mathrm{GeV}$ is huge, it is still much smaller than the Planck mass $M_{\mathrm{Pl}} \sim 10^{19}\,\mathrm{GeV}$, which is thought to be the scale where on the one hand, gravity can be no longer described classically, and on the other hand, the actual quantum description is not known. Therefore, the new physics indicated by presence of the Weinberg operator is expected to be in the regime where gravity is not quantized.

### 1.2.2 Dark matter

The evidence of the second phenomenon beyond the Standard Model was found outside the Earth, and is related to the existence of the so-called **Dark Matter** (DM). Dark matter manifests itself via different independent types of observations, at very different lengthscales, starting from changing the motion of stars [22] and galaxies, and up to the cosmological scales, affecting formation of large-scale structures and dynamics of the Universe as a whole [23].

[1] Otherwise, at higher energies, the unitarity of the scattering matrix is lost, so that some scattering processes can have probability larger than 1, which makes theory inconsistent.

There are three independent traces of gravitational potential in astrophysical systems (velocity curves of stars and galaxies, X-ray emission of intergalactic gas and gravitational lensing [24]) that all show that **gravity in these objects deviates significantly from what is predicted for the observed distributions of ordinary matter by Newton's (or, equally Einstein's) theory of gravity**. Independently, the observed properties of CMB suggest that without an additional component that does not interact with light, ordinary matter would not have enough time to develop all the structure observed in the Universe at the present day [25, 26, 27]. This body of independent evidence suggests that some additional matter, called *Dark Matter* really exists.

In all these cases, however, the only way DM manifests itself is through gravitational interactions with ordinary matter. The origin of this effect can be either in the existence of massive particles that are not involved in the SM gauge interactions (then indeed we deal with "matter"), or in modifications of the laws of gravity. The attempts to modify the gravitational laws at large scales encounter many problems, both from theoretical and experimental sides. The scenario where the DM is composed of particles is simple, natural and universal (for a review, see [28, 29]).

But if the Dark Matter is made of new particles, which particles are they? Can we find them?

Although the Dark Matter constitutes the majority of the matter in the Universe, there is no suitable candidate in the Standard Model that can play a role of the DM particle. At first sight, neutrinos seem to look promising but actually they cannot constitute more than few percent of Dark Matter. Indeed, assuming that all existing particles and interactions are described by the SM, we can unambiguously calculate the number density of relic neutrinos at the present epoch. If the mass of these particles is too large, the contribution to energy density would be too large as well. This gives an *upper* bound on the mass of the "DM neutrino". On the other hand, the astrophysical observations of dwarf galaxies, which are DM-dominated compact objects, show that if the Dark Matter particle is a fermion, then its mass should exceed several hundred eV (otherwise, the number phase space density of the particles would have to exceed that of a degenerate Fermi gas and violate the Pauli principle to explain the observed mass distributions in these objects) [30, 31]. This gives a *lower* bound. Therefore, cosmological and astrophysical requirements for the properties of SM neutrinos to serve as the DM particle *contradict to each other*.

Moreover, we know now from particle physics experiments that the masses of SM neutrinos can not exceed a few eV. For such small particle masses, the structure formation would proceed in a qualitatively different way, with large objects forming earlier than the small ones, which contradicts observations [27, 32]. The data on the abundances of primordial elements and on the properties of the Cosmic Microwave Background also confirm independently that the contribution of neutrinos to the present-day energy density is very small [20, 33]. Thus we can robustly conclude that the SM by itself does not explain Dark Matter and some new physics is required.

### 1.2.3 Matter-antimatter asymmetry of the Universe

The third BSM problem that we want to mention is related to the observation that **we live in a world filled almost exclusively by matter, with no significant traces of primordial antimatter**.

Let us go back in time, to when the Universe was hot. At high enough temperatures, particles that constitute the matter were relativistic, and were produced in particle-antiparticle pairs. Therefore, the individual densities of baryons $n_B$ and anti-baryons $\bar{n}_B$ were not conserved, only their asymmetry was conserved, $n_B - \bar{n}_B$. The densities of relativistic particles are comparable to each other, therefore $n_B \sim n_\gamma$ (density of photons).

All pairs later annihilate to the photons and therefore the asymmetry at later times is characterised by the so-called baryon-to-photon ratio. This quantity affects a number of observables and therefore its present-day value is known relatively well [34]:

$$\eta_B = \frac{n_B - \bar{n}_B}{n_\gamma} = (6.047 \pm 0.074) \times 10^{-10}, \tag{1.2}$$

The quantity $\eta_B$ does not change with time, up to the temperatures of about 100 GeV. This property is called the Baryon Asymmetry of the Universe (BAU).

Although $\eta_B$ is small, it requires an explanation, since if the theory possesses exact symmetry between particles and anti-particles, $\eta_B$ would never change during the evolution. In such a theory, the only way to have non-zero $\eta_B$ would be to postulate it as an initial condition. Indeed, our description of the Universe based on the hot Big-Bang cosmology cannot be extended arbitrary far into the past, not only because for high enough temperatures we do not have observational data, but also because we cannot trust the Standard Model anymore (indeed, for energies which are close to the Planck scale, we do not know what is the correct physical description of the Universe). Therefore, maybe the value of the baryon asymmetry is given by initial conditions?

However, if the flatness of the Universe, the initial spectrum of density perturbations (required for development of the observed large-scale structure) and other observed properties of the Universe are explained by an epoch of rapid accelerated expansion (the model of cosmological inflation [35, 36, 37], that is well motivated by the data and has no compelling alternatives at present [38]) – this scenario becomes very unlikely. Indeed, in the inflationary picture all the densities of all charges, including the baryon asymmetry, would be diluted by a very huge factor like $e^{-60}$, and at the beginning of the post-inflationary stage, all the initial conditions would be “forgotten” [39]. All subsequent dynamics should be governed by the SM, or we should assume the existence of some new particle physics. Regardless, we need a particle physics mechanism that would explain the change of $\eta_B$ and, therefore, introduce some asymmetry between particles and antiparticles at a fundamental level. In principle, such a mechanism could exist in the SM (the so-called electro-weak baryogenesis) if the spontaneous breaking of the electroweak symmetry would go through a first-order phase transition, which requires the mass of the Higgs boson below 70 GeV [40, 41, 42]. However, since the time of the Large Electron Positron (LEP) collider experiment, we know the mass of the Higgs boson should above 114GeV [43] (according to the LHC data, the mass is 125GeV [44, 45]). Therefore the electroweak baryogenesis should not take place in the early Universe, and we face a real BSM problem here.

In order to explain the abovementioned observational BSM problems, researchers come up with new theories. These theories, on the one hand, should reproduce the behaviour of the Standard Model, which was confirmed in the numerous past experiments, and on the other hand, provide new particles and interactions that are responsible for the new physics.

### 1.2.4 Approaches to resolve the BSM problems

"BSM model-building" can be roughly divided into two types: the "top-down" and "bottom-up" approaches. In the top-down approach, one attempts to guess the correct theory, which is based on a new physical principle (among the representative examples are supersymmetric theories, theories with extra dimensions and string theory). To guess the correct fundamental principle one may use as a criterion "naturalness", by trying to explain certain peculiar properties of the SM (hierarchy problem, strong CP-problem etc), or even try to solve a more fundamental problem, e.g. to build a theory of quantum gravity. Solutions to the observational BSM problems typically appear as possible by-products of the postulated fundamental principle. Sometimes the richness of the top-down models becomes their phenomenological drawback, as it is very challenging to falsify the whole class of models based on the same fundamental principle (like, for example, the whole class of supersymmetric extensions of the SM).

The bottom-up approach concentrates on the solution of the BSM problems, by building a theory, falsifiable with available experimental means. If such a theory is confirmed experimentally, one would then start to explore its structure, such as hidden symmetries underlying small parameters, etc. Since the abovementioned BSM phenomena are apparently unrelated, once we have a theory that explains them all simultaneously, a number of non-trivial independent experimental checks becomes available. *In what follows we will concentrate on the bottom-up approach.*

## 1.3 Sterile neutrinos and the $\nu$MSM model

*In the bottom-up approach, an interesting possibility to solve several BSM problems is provided by the* ***right-handed*** *neutrino.* We have already noticed above that, in the SM, neutrinos can be only left-handed. However, a more precise statement would be that if we add right-handed neutrinos to the SM, these particles will not interact through electromagnetic, weak or strong forces and, therefore, will not affect the confirmed phenomenology of the Standard Model. These right-handed particles are usually called "sterile" neutrinos, and in this context the usual neutrinos are called "active". More formally, "sterile" means that the fields $N_I(x)$ of right-handed neutrinos are singlets under the $U_Y(1) \times SU_L(2) \times SU_C(3)$ gauge group of the Standard Model, therefore sterile neutrinos are sometimes called singlet neutrinos.

Once we include a right-handed neutrino $N$ to the spectrum of particles, the so-called Yukawa coupling

$$\Delta\mathcal{L}_Y = -F\bar{L}(x)\tilde{H}(x)N(x) + \text{h.c.}, \tag{1.3}$$

between left ($L$) leptons, right neutrinos and the Higgs field $H$ is possible (we use the same notation as before, $\tilde{H} = i\sigma_2(H^\dagger)^T$). After the spontaneous symmetry breaking, this term has the form of the "Dirac mass" $M_D\bar{\nu}N$.[2] This way, left-handed neutrinos receive mass, which is the same as the mass of the right-handed partner. Here, we have considered for simplicity only one lepton generation and one singlet neutrino, but the numbers of left and right particles can be easily extended so that oscillations between different active flavours may take place. In this scenario, neutrinos are Dirac particles, the masses of sterile neutrinos are the same as the masses of active neutrinos, and are very small according to the observations.

However, neutrinos should not be necessarily Dirac particles. Instead, since right-handed neutrinos are neutral, they can carry no conserved quantum number (like the lepton number), so that the additional term becomes possible,

$$\Delta\mathcal{L}_{\text{Maj}} = -\frac{M_s}{2}\overline{N^c}N + \text{h.c.}, \tag{1.4}$$

the so-called Majorana mass term, where $M_s$ is the Majorana mass of the particle. Since right-handed neutrinos are singlets, the Majorana mass term does not violate the gauge symmetry of the SM, in contrast to the Majorana mass term $m_\nu\overline{\nu^c}\nu$ for left-chiral neutrinos. If we consider singlet neutrinos, which have both the Dirac $M_D$ and Majorana $M_M$ masses, then neither of the flavour eigenstates $\nu$ and $N$ has a definite mass. In other words, mass eigenstates $N_M$, $\nu_M$ do not

[2] Note that the coupling of neutrinos to the Higgs field in (1.3) is important, since $L(x)$ is a two-component field ($SU_L(2)$-doublet), and it transforms non-trivially under $SU_L(2)$ transformations. Recalling that $N$ does not transform under $SU_L(2)$, one concludes that the simple combination $\bar{L}N$ is not gauge-invariant, so that presence of this term would make the extension of the SM self-inconsistent. On the other hand, the combination $\bar{L}HN$ *is* gauge-invariant.

coincide with the flavour eigenstates. Instead, the two bases are related by a $2 \times 2$ unitary transformation, which can be reduced to an orthogonal matrix (by a phase redefinition of the fields $\nu(x)$, $\nu_M(x)$, $N(x)$, and $N_M(x)$),

$$\begin{pmatrix} \nu_M \\ N_M \end{pmatrix} = \begin{pmatrix} \cos\theta & \sin\theta \\ -\sin\theta & \cos\theta \end{pmatrix} \begin{pmatrix} \nu \\ N \end{pmatrix} \tag{1.5}$$

The real-valued parameter $\theta$ describes the quantum-mechanical mixing between the flavour and mass eigenbases, and is usually called the *mixing angle*. In what follows, we concentrate on the particular case of small Dirac mass, $M_D \ll M_M$. Then, as a result of diagonalization of the Lagrangian with Dirac and Majorana terms, the mixing angle is found to be

$$\theta = \frac{M_D}{M_s} \ll 1, \tag{1.6}$$

the lighter mass eigenstate $\nu_M$ is close to the active flavour eigenstate $\nu$, and it has mass

$$m_\nu \sim \frac{M_D^2}{M_s}. \tag{1.7}$$

The heavier mass eigenstate $N_M$ is close to the sterile flavour eigenstate $N$, and has mass approximately equal to $M_s$.

If singlet neutrinos are neutral with respect to the SM gauge group, then how do these particles interact with ordinary matter at all? The interaction is described in Fig. 1.1: although sterile neutrinos do not interact directly, they couple to active neutrinos via the Dirac mass, so that a sterile neutrino can trasform into an active neutrino with probability proportional to the squared mixing angle, $\theta^2$. Therefore, we conclude that sterile neutrinos interact with the effective coupling constant $\theta G_F$, where $G_F$ is the Fermi constant.

If we consider energies $E$ much smaller than the Majorana mass, $E \ll M_s$, then the singlet state is not produced as a real particle, and the effective interaction of active neutrinos is described by

$$\mathcal{L}_{\rm mass} = \frac{F^2}{M_s} (\bar{L}\tilde{H})(H^\dagger L^c), \tag{1.8}$$

which is illustrated at the level of Feynman diagrams in Fig. 1.2. One recognizes in $\mathcal{L}_{\rm mass}$ the Weinberg operator (1.1), if one identifies $\Lambda$ with $M_s$.

By looking at (1.7), we can note two important things. First, for $M_D \ll M_s$, the active neutrino mass $m_\nu$ can be arbitrary small, $m_\nu \ll M_D$, for any $M_D$. This explanation of the smallness of the observed neutrino masses (which are below eV) is usually referred to as the "see-saw" mechanism [46, 47, 48, 49]. Second, in neutrino oscillation experiments we measure two independent combinations of neutrino masses $m_i$, namely $m_1^2 - m_2^2$ and $m_1^2 - m_3^2$. This means that we need at

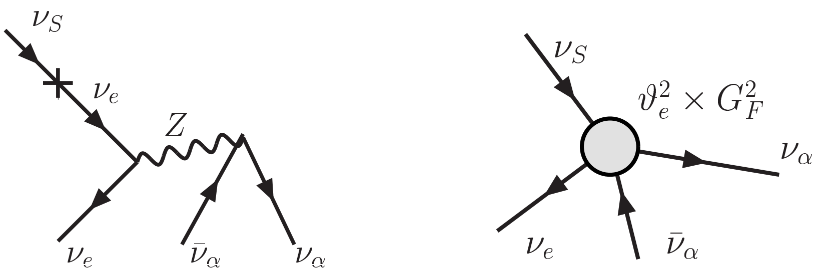


(a) Decay of sterile neutrino $\nu_S \to \nu_e \nu_\alpha \bar{\nu}_\alpha$ through neutral current interactions

(b) Fermi-like interaction with the "effective" Fermi constant $\vartheta_e \times G_F$ for the process in the panel (b).

Figure 1.1: Fermi-like super-weak interactions of sterile neutrino

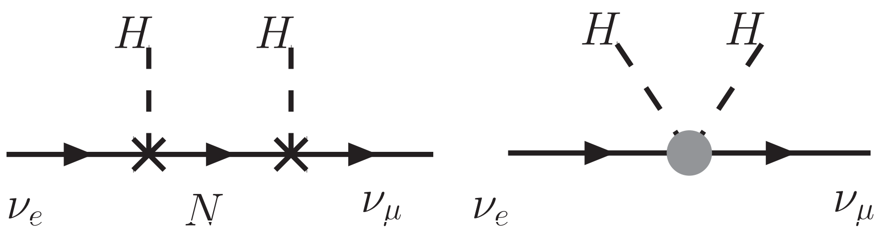


Figure 1.2: Neutrino oscillation $\nu_e \to \nu_\mu$ is mediated by sterile neutrino $N$ (left panel). At low energies, the sterile neutrino line shrinks to a point, so that the local Weinberg operator appears (right panel). In both panels, $H$ is the Higgs field.

least two singlet neutrinos to explain the observations, in which case the lightest active neutrino mass eigenstate is massless [50]. But the absolute value of these neutrino masses is not fixed by the data and if the smallest neutrino mass is different from zero, the minimal number of right-handed neutrinos, needed to explain neutrino flavour oscillations, will be three.

For an arbitrary number of right-handed neutrinos the Lagrangian of the corresponding extension of the SM will be then

$$\mathcal{L} = \mathcal{L}_{\rm SM} + i\bar{N}_I \gamma^\mu \partial_\mu N_I - \left( F_{\alpha I} \bar{L}_\alpha N_I \tilde{H} + \frac{M_I}{2} \overline{N_I^c} N_I + \text{h.c.} \right). \tag{1.9}$$

Here the sum over the indices of sterile neutrinos $I$ and over the flavour indices $\alpha$ is understood, and $\mathcal{L}_{\rm SM}$ is the Lagrangian of the Standard Model. In the case of three right-handed neutrinos we have equal numbers of right-handed (sterile) and left-handed (active) neutrinos of the SM and the symmetry between left and right fermions is restored, see Fig. 1.3. Moreover, it turns out that this number

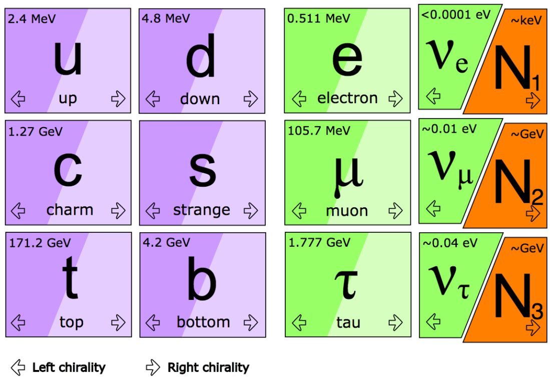


Figure 1.3: The Standard Model extended with three right-handed (sterile) neutrinos, $N_1, N_2$, and $N_3$.

is enough to explain all the three abovementioned BSM problems, as we discuss below.

In the case of three sterile neutrinos, the see-saw relation (1.7) is generalized to

$$\hat{m}_\nu = \hat{M}_D \operatorname{diag}\left(\frac{1}{M_1}, \frac{1}{M_2}, \frac{1}{M_3}\right) \hat{M}_D^T, \tag{1.10}$$

where $\hat{m}_\nu$ is the $3 \times 3$ mass matrix of active neutrinos, $(\hat{M}_D)_{\alpha I} = F_{\alpha I} v$ is the matrix of Dirac masses. According to this formula, the absolute scale of Majorana masses of sterile neutrinos is not fixed. These masses can be as large as $10^{15}$ GeV, or they can be very small, in principle.

In what follows, we consider a model where there are right-handed (sterile) neutrinos that have masses below the electroweak scale of 100 GeV, so that **no new high-energy scale is added to the Standard Model.** In this case the mixing angles are small and these particles are very hard to observe at accelerators. They do not change the phenomenology of previous experiments and special strategy should be implemented to detect them (see below). **Their role in cosmology, however, can be profound. Indeed, the small probability of interactions can be overcome by the high density of the SM particles in the extreme conditions of the early Universe.**

### 1.3.1 Sterile neutrinos in the early Universe

To describe the dynamics of sterile neutrinos in the early Universe let us recall that their interaction with the SM matter goes through mixing with active neutrinos. *The properties of active neutrinos are modified (renormalized) in the presence of* *the dense medium of the hot Universe and, therefore, the active-sterile mixing is modified as well.* Indeed, a probe neutrino that propagates through a medium, interacts weakly with all the particles of this medium, and if we average statistically over these interactions, the usual Dirac equation,

$$i\partial_\mu \gamma^\mu \nu(x) = 0 \tag{1.11}$$

which describes neutrinos in vacuum, is modified in presence of medium,

$$(i\partial_\mu \gamma^\mu - \Sigma)\nu(x) = 0. \tag{1.12}$$

The neutrino gets "dressed" by medium, and the effect of dressing is described by the self-energy $\Sigma$, which has the form [51]

$$\Sigma = \gamma^0 \left[ b \frac{G_F}{M_W^2} p T^4 + c\, G_F (n_L - \bar{n}_L) \right], \tag{1.13}$$

where $n_L$ and $\bar{n}_L$ are the equilibrium densities of leptons and antileptons, respectively. The dimensionless coefficients $b$ and $c$ depend on the particle content of the plasma, and on the neutrino flavour, but regardless both of them are of order 1. Neutrinos with different momenta $p$ get dressed differently, therefore $\Sigma$ is momentum-dependent.

The presence of self-energy in the modified Dirac equation (1.12) indicates that the dispersion relation of neutrinos in medium is modified,

$$E(p) = p + V, \tag{1.14}$$

where the quantity

$$V = V(p, T) \equiv \gamma^0 \Sigma \tag{1.15}$$

has the meaning of effective potential of the particle in plasma. This potential depends both on temperature and particle momentum. Since the presence of a medium introduces a preferred frame of reference (the one where the plasma is at rest as a whole), the dispersion relation (1.14) no longer has a Lorentz-covariant form. It implies that if we define mass $m_\nu$ of neutrino through $m_\nu^2 = E^2 - p^2$, then we find that neutrinos with different momenta have *different* masses.

We define the *effective* mixing angle $\theta$ in medium through

$$\hat{H} = \begin{pmatrix} \cos\theta & -\sin\theta \\ \sin\theta & \cos\theta \end{pmatrix} \begin{pmatrix} E_1 & 0 \\ 0 & E_2 \end{pmatrix} \begin{pmatrix} \cos\theta & \sin\theta \\ -\sin\theta & \cos\theta \end{pmatrix}, \tag{1.16}$$

where

$$\hat{H} \equiv \begin{pmatrix} \cos\theta_0 & -\sin\theta_0 \\ \sin\theta_0 & \cos\theta_0 \end{pmatrix} \begin{pmatrix} p & 0 \\ 0 & \sqrt{p^2 + m_N^2} \end{pmatrix} \begin{pmatrix} \cos\theta_0 & \sin\theta_0 \\ -\sin\theta_0 & \cos\theta_0 \end{pmatrix} + \begin{pmatrix} V & 0 \\ 0 & 0 \end{pmatrix} \tag{1.17}$$

is the effective Hamiltonian of active and sterile neutrinos in medium. Here we write the Hamiltonian in the flavour eigenbasis. In other words, $\theta$ describes the relation between flavour and mass eigenstates in medium.[3] The first term on the right-hand side of Eq. (1.17) is the same as in vacuum, and tells us that the vacuum mass eigenstates are related to vacuum flavour eigenstates by a rotation with angle $\theta_0$, according to Eq.(1.5) (the subscript 0 indicates here that the mixing angle corresponds to zero temperature). The second term on the right-hand side, however, is the medium correction. This correction is present only for the active flavour eigenstate, since sterile flavour eigenstate does not interact directly via weak interactions.

At finite temperature, the effective mixing angle $\theta$ is different from the vacuum mixing angle, and the diagonalization of the effective Hamiltonian shows

$$\theta = \theta(T) \approx \arctan\left[\theta_0 \, \frac{2\Delta E_{\rm vac}}{\Delta E_{\rm vac} + V + \sqrt{(\Delta E_{\rm vac} + V)^2 + 4\theta_0^2 \Delta E_{\rm vac}^2}}\right], \quad (1.18)$$

Temperature dependence enters through the potential $V$ (1.15). Here $\Delta E_{\rm vac} = m_N^2/2p$ is the difference of energies for active and sterile neutrinos in vacuum, for a given common momentum $p$. At non-zero temperature, however, this difference of energies is modified,

$$\Delta E(p) \equiv E_2(p) - E_1(p) = \sqrt{(\Delta E_{\rm vac} + V)^2 + 4\theta_0^2 \Delta E_{\rm vac}^2}. \quad (1.19)$$

Since active neutrinos are in thermal equilibrium at high temperatures, most of them have momentum $p \sim T$. As a consequence, sterile neutrinos have momenta in the same range.

In absence of lepton asymmetry, $n_L - \bar{n}_L = 0$, the mixing angle increases monotonically with lowering the temperature, and reaches the maximal value at zero temperature, $\theta = \theta_0$, see the left panel in Fig. 1.4. Therefore, in this case the mixing angle remains small all the time.

In presence of lepton asymmetry, however, the behaviour of the mixing angle changes. First, the temperature dependence of the mixing angle is non-monotonic anymore, and second, mixing angle can reach large values, $\theta \sim 1$. (See the right panel in Fig. 1.4.) This large value of the mixing happens when $\Delta E_{\rm vac} + V = 0$, and according to (1.19) it is accompanied by suppression of the energy splitting $\Delta E$. It means that levels of active and sterile neutrinos almost cross each other, so that *resonance* happens.

In order to find the interaction rate $\Gamma_N$ of sterile neutrinos in medium, one can use the estimate $\Gamma_N \sim n\sigma_N$, where $n$ is the concentration of the SM particles, $\sigma_N$ is the cross-section of a typical reaction with sterile neutrino, for example $N + \nu \to \nu + \nu$. Concentrations of relativistic particles are $n \sim T^3$, and the cross-section of sterile neutrino is the same as for active neutrino, only the additional

[3] In agreement with what was said above about the neutrino mass in medium, by "mass eigenstates" in medium we mean states that have definite energy for a given momentum.

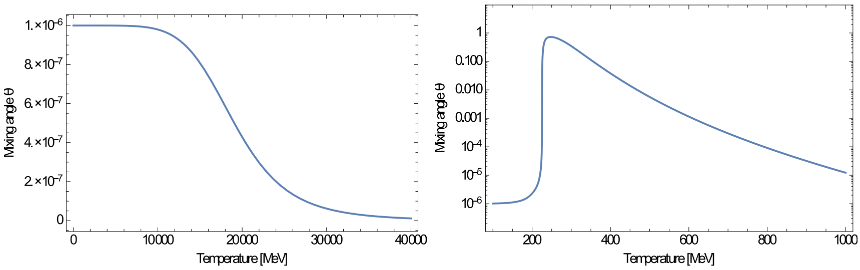


Figure 1.4: Temperature dependence of active-sterile mixing angle. Left panel: $M_s = 1$ GeV, no lepton asymmetry. Right panel: $M_s = 10$ keV, the ratio of the lepton number $L$ to the entropy $S$ is $L/S = 10^{-5}$. In both panels, the vacuum mixing angle is $\theta_0 = 10^{-6}$, the neutrino energy is equal to temperature, $E = T$.

suppression factor $\theta^2$ is added, $\sigma_N \sim \theta^2 G_F^2 T^2$. Therefore,

$$\Gamma_N \sim \theta^2(T) G_F^2 T^5. \tag{1.20}$$

If the interaction rate $\Gamma_N$ is much smaller than the Hubble expansion rate $H(T)$, then singlet neutrinos do not reach thermal equilibrium. In other words, if the Universe expands faster, than the interactions take place, the particles do not have time to come into equilibrium with the rest of the plasma.

From the Friedmann equation $H^2 = 8\pi\rho/3M_{\text{Pl}}^2$, the Hubble rate can be estimated as

$$H(T) \sim \frac{T^2}{M_{\text{Pl}}}. \tag{1.21}$$

Here $M_{\text{Pl}} \approx 1.2 \times 10^{19}$ GeV is the Planck mass, and $\rho \sim T^4$ is the plasma energy density.

If we neglect the temperature dependence (1.18), then at some sufficiently high temperature the interaction rate (1.20) becomes larger than the expansion rate (1.21). However, the temperature dependence of the mixing angle invalidates this conclusion. Instead, the ratio $\Gamma_N/H$ has a peak at some temperature, as it is illustrated in Fig. 1.5.

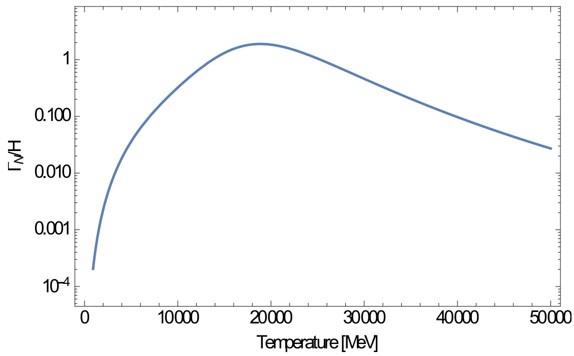


Figure 1.5: Temperature evolution of the ratio $\Gamma_N/H$ of the sterile neutrino production rate $\Gamma_N$ to the Hubble expansion rate $H$. $M_s = 1$ GeV, vacuum mixing angle is $\theta_0 = 10^{-6}$, no lepton asymmetry is present in the Universe. The energy of sterile neutrino is equal to temperature, $E = T$.

The two different scenarios for the evolution of sterile neutrinos in the early Universe are possible.

1. Although the mixing angle is much smaller than 1, the rate of interactions $\Gamma_N$ can exceed the expansion rate at some temperature, $T = T_+$, and sterile neutrino reaches thermal equilibrium. At smaller temperatures, the interaction rate decreases faster than the expansion rate, so at some point ($T = T_-$) sterile neutrinos fall out of equilibrium.

2. The mixing angle is so small, that thermal equilibrium of $N$ is never reached. In this case, the sterile neutrino number density $n_N$ is smaller than the equibrium value, $n_N < n_{\text{eq}} \sim T^3$, but anyway this density can be significant, especially at the later stages of the Universe evolution, as we will see below.

The ratio $\Gamma_N/H$ for the first scenario is plotted in Fig. 1.5. For the second scenario, when $\Gamma_N \ll H$ all the time, the density of sterile neutrinos can be estimated very roughly as

$$\frac{n_N}{n_{\text{eq}}} \sim \left(\frac{\Gamma_N}{H}\right)_{\text{Max}} \sim \theta_0^2 M_s M_{\text{Pl}} G_F^{3/2} M_W \simeq \frac{\theta_0^2}{10^{-13}} \frac{M_s}{\text{GeV}} \quad \text{(No lepton asymmetry)} \tag{1.22}$$

in absence of lepton asymmetry. Here we have noticed that the ratio $\Gamma_N/H$ peaks around the temperature

$$T \sim \left(\frac{M_W^2 M_s^2}{G_F}\right)^{1/6} \simeq 10\,\mathrm{GeV} \times \left(\frac{M_s}{\mathrm{GeV}}\right)^{1/3}, \tag{1.23}$$

where the terms $\Delta E_{\mathrm{vac}}$ and $V$ in Eq. (1.18) are of the same order.

Here one has to distinguish number density $n_N$ and energy density $\rho_N$. Even if the number of sterile neutrinos is much smaller than the number of SM particles, $n_N \ll T^3$, it does not mean that they do not contribute to the energy density. Indeed, although sterile neutrinos are produced relativistic, their momenta get smaller with the Hubble expansion, due to the gravitational redshift. It means that if their mass is sufficiently large, these particles can become non-relativistic at some point, and their energy density $\rho_N \sim n_N M_s$ can become comparable to the energy density of SM particles, $\rho_{\mathrm{SM}} \sim T^4$.

For the resonantly produced sterile neutrinos, their density has the same order of magnitude as the density of lepton number,

$$n_N \sim n_L - \bar{n}_L \quad \text{(Large lepton asymmetry)} \tag{1.24}$$

Indeed, sterile neutrinos are produced relativistic, which means that the mass is not important for them. For neutrinos, which are almost massless, the active+sterile lepton number (the SM lepton number plus number of left-helical sterile neutrinos minus number of right-helica sterile neutrinos) is conserved during the oscillations and collisions. The effective resonant production implies then that the significant fraction of SM lepton number was transferred to the "sterile lepton number".

In case when sterile neutrinos do not reach thermal equilibrium, their out-of-equilibrium abundance is different in the two cases:

1. If lepton asymmetry is absent, the effective mixing angle does not exceed its vacuum value $\theta_0$, and the abundance is suppressed by $\theta_0^2$ (non-resonant production).

2. If lepton asymmetry is present, resonant enhancement of the effective mixing angle can happen, the abundance of sterile neutrinos is not suppressed by $\theta_0^2$, and is proportional to lepton asymmetry (resonant production).

As we have noticed above, extensions of the Standard Model should explain all the previous experiments, which were expained by the SM. Similarly, the well-established cosmological phenomena, which were explained by the SM, should not change in these extensions as well. For example, the SM describes very good the so-called Big-Bang Nucleosynthesis (BBN), which is essentially the epoch, when the first light nuclei are formed out of the initial neutrons and protons (see reviews [52, 53, 54]). Theoretical predictions of the SM are in nice agreement with the astrophysical observations of the relic abundances of light nuclei such as $^2$H, $^3$He, and $^4$He [52]. If the Standard Model is extended with sterile neutrinos, this agreement should not be lost.

What is the influence of sterile neutrinos on the BBN? First, presence of sterile neutrinos increases the energy density of plasma, and according to the Friedmann equations, it increases the expansion rate of the Universe. Second, sterile neutrinos introduce deviation from thermal equilibrium, so that spectra of active neutrinos are distorted, the rate of weak reactions is altered, and the moment when neutrons fall out of equilibrium is shifted (this moment is crucial, since it defines the ratio of concentrations of neutrons and protons at the onset of the BBN).

In order not to spoil the agreement between the SM predictions of the Big-Bang Nucleosynthesis and observations, sterile neutrino should be either long-lived and be present in negligible amount in plasma, or to be short-lived, and to decay before the nucleosynthesis starts. If sterile neutrinos describe neutrino oscillations, their mixing angles are large enough so that the scenario with long-lived particles does not take place for them. **The impact on the nucleosynthesis of such sterile neutrinos is discussed in detail in Chapter 3**.

Having discussed the potential importance of sterile neutrino in the early Universe, below we will discuss in detail how this particle can play a role of Dark Matter, and how it can give rise to the Baryon Asymmetry of the Universe.

### 1.3.2 Sterile neutrino Dark Matter

It is known that sterile neutrino $N$ with mass in the keV region is a viable Dark Matter candidate [55, 56, 57]. Then, this neutrino has to be stable on the cosmological timescales, or equivalently, its lifetime should exceed the age of the Universe. **Therefore, $N$ has a small mixing angle.**

Moreover, if we return to the previous discussion of the dynamics of sterile neutrino in the early Universe, we can conclude that the mixing angle should be small enough for sterile neutrino *not to* reach equilibrium in the early Universe. Indeed, if our DM particle went through the equilibrium period, its number density $n_N$ would be comparable to the number density of photons or ordinary neutrinos or be even larger. Therefore, like for active neutrinos, to give the correct DM mass density, the mass of sterile neutrino with such a number density would have to be $M_s \simeq 10\,\text{eV}$ (see e.g. [33]). Exactly like for ordinary neutrinos, this number would contradict the Pauli principle applied to DM-dominated astrophysical objects (Tremaine-Gunn bound [30]), which implies that $M_s \gtrsim 400\,\text{eV}$ [31]. Therefore, the DM sterile neutrinos should be out of thermal equilibrium at all temperatures and therefore their number density is suppressed as compared to the number density of ordinary neutrinos or photons, and mass can be in keV range (or it can be even larger).

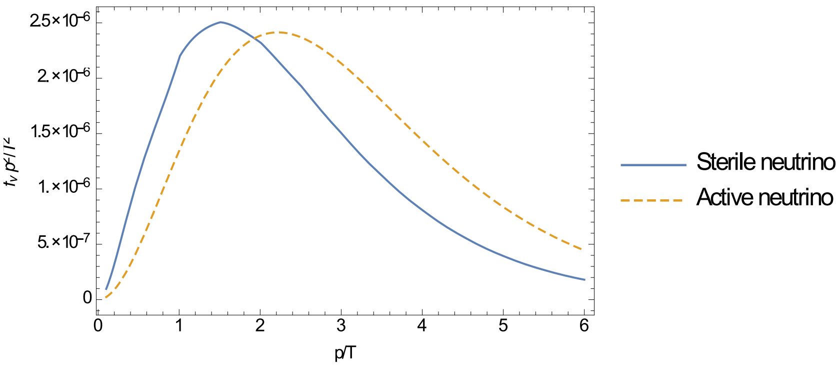


Figure 1.6: Comparison of sterile neutrino distribution function $f_s(p)p^2/T^2$ and the equilibrium Fermi distribution $f_{\rm Fermi}(p)p^2/T^2$ ($p$ is the particle momentum, $T$ is temperature). The mass of sterile neutrino is $M_s = 10\,\mathrm{keV}$, the vacuum mixing angle is $\theta_0 = 10^{-6}$, lepton asymmetry is absent. The absolute scale of the Fermi distribution is reduced so that the two spectra vary in the same range.

According to the estimate (1.23), the dominant fraction of DM particles with keV mass is produced around the temperature $T \sim 100$ MeV. Therefore (in absence of lepton asymmetry, see below) their spectrum has form that is close to the equilibrium Fermi-Dirac distribution with this temperature (that decreases as the Universe expands) [55] (see Fig. 1.6), although the normalisation of spectrum is smaller than 1, as the thermal equilibrium was not established.

As it was already discussed above, a different scenario takes place in presence of lepton asymmetry. In this case a resonant enhancement of the effective mixing angles takes place. This resonant production [56, 58] requires smaller vacuum mixing angles to produce the correct DM abundance for the same particle mass, than the non-resonant production described above. In the resonant case the shape of the spectra of resonantly produced sterile neutrinos can deviate significantly from the Fermi distribution [58, 59] (if the lepton asymmetry is large enough, i.e. comparable with the number of DM particles), see Fig. 1.7. In both resonant and non-resonant cases production of Dark Matter particles happens at temperatures $T \lesssim$ GeV [58, 60, 61].

Of course, here we assume (in the spirit of bottom-up approach) that sterile neutrinos are produced only from their mixing with ordinary neutrinos. If some other new particles exist, apart from sterile neutrinos, there can be more mechanisms of the sterile neutrino DM production. We do not consider these models here.

If DM particle is a sterile neutrino, this particle has so small mixing angle that its contribution to the active neutrino masses is negligible (see e.g. [62]).

The Dark Matter particle can be searched in the cosmic X-ray emission [63, 62]. Although $N$ is stable on cosmological scales, it nevertheless decays. The life time

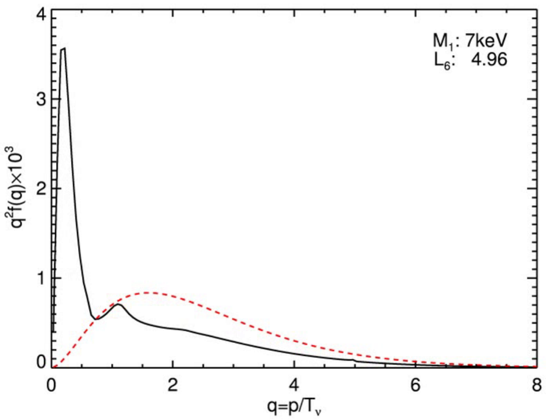


Figure 1.7: Sterile neutrino DM distribution function $f_s(q)q^2$ ($q = p/T$, where $p$ is the particle momentum, $T$ is the temperature). The solid line corresponds to resonantly produced sterile neutrino with initial ratio of lepton asymmetry to entropy equal to $4.5 \times 10^{-5}$. The dashed line is the spectrum of non-resonantly produced sterile neutrino. The mass of sterile neutrino in both cases is $M_s = 7$ keV.

of this particle is defined by the dominant tree-level three-body decay channel $N \to \nu\nu\bar{\nu}$. There exists also a radiative two-particle decay channel into neutrino and photon, $N \to \nu\gamma$. This decay channel is sub-dominant [64], since it involves a combination of weak and electromagnetic processes at one loop. Although the life time with respect to this decay channel is even longer than for the previous one (and therefore is much longer than the life time of the Universe), the photons emitted in this way can in principle be produced in detectable amounts, due to very large number of DM particles in DM-dominated astrophysical objects. As this is a two-body decay into (almost) massless particles, the energy of the emitted photons is *fixed*, and is equal to one half of the sterile neutrino mass. This property implies a peak in the X-ray spectrum of Dark-Matter dominated regions of space [65, 66]. (The peak is smeared only slightly, by the Doppler effect, caused by the velocity dispersion of Dark Matter particles.)

Recently, an unidentified 3.5 keV line was found in the spectrum of X-rays [67, 68]. The behaviour of this line is consistent with the DM origin: in DM-dominated regions of space, the signal is stronger, in regions with low DM abundance the signal is not found. Therefore, it may be an indication of Dark Matter decay. If this signal comes from decays of DM sterile neutrinos, it should be resonantly produced, implying large enough lepton asymmetry at the temperatures $T \lesssim$ GeV [59, 60, 61].

X-ray bounds show that for both resonant and non-resonant production the mass of DM sterile neutrino should be in the keV range (assuming no other new physics at the relevant temperatures). Therefore, these particles are produced relativistic and have significant *free-streaming length*. This means that the structure formation will be suppressed at the smaller scales as compared to the Cold Dark Matter case (DM particle created non-relativistic). Although sterile neutrino Dark Matter has non-thermal primordial velocity distribution, it is clear that for the smaller masses the effect of free-streaming will be stronger (see Fig. 1.8) and therefore cosmological observations could provide a *lower bound* on Dark matter mass (for each given lepton asymmetry), while X-ray observations provide upper bounds. Free-streaming scales corresponding to DM particles with masses in keV range are such that, for example, CMB observations are not sensitive to them. Cosmological lower bounds require complicated non-linear analysis of structure formation at small scales, subject also to uncertainties related to (largely unknown) baryonic physics. Although promising, this approach requires a lot of additional work to be done. Nevertheless, for the case of the non-resonantly produced sterile neutrino DM, the contradiction between astrophysical X-ray upper bound and cosmological lower bound on DM mass is rather strong (see [69, 70, 71]) and, even with all uncertainties of the method taken into account, this scenario should be considered as strongly disfavoured by the data. For resonantly produced sterile neutrino, however, both cosmological and astrophysical bounds are weaker, leaving enough room for sterile neutrino DM to be produced from interactions with the SM particles [72].

The Dark Matter is made of sterile neutrinos produced from interactions with the SM plasma, the observational bounds imply that they have to be produced resonantly. This requires lepton asymmetry, which is much larger than the baryon asymmetry, to be present at temperatures $T \lesssim$ GeV.

### 1.3.3 Generation of the baryon asymmetry with sterile neutrinos

It turns out, that sterile neutrinos can not only explain neutrino oscillations and serve as a Dark Matter candidate, but can also generate the Baryon Asymmetry of the Universe, as we discuss below.

In general, to generate the baryon asymmetry, three conditions (the "Sakharov conditions") should be satisfied [75]

1. Baryon number is not conserved
2. C- and CP-symmetries are violated
3. The Universe must be out of thermal equilibrium during the process of generation of the baryon asymmetry

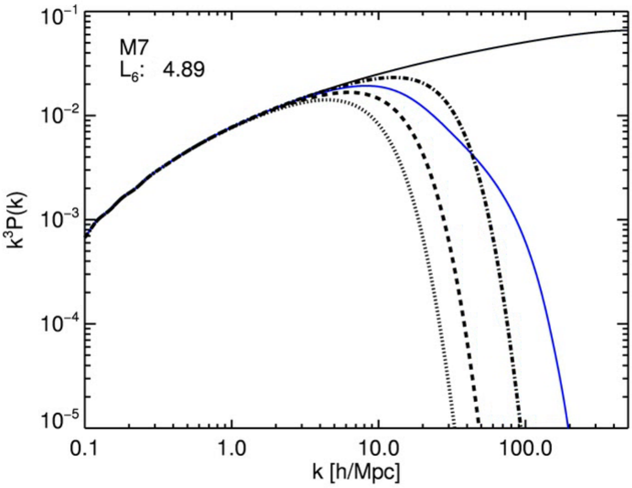


Figure 1.8: Power spectrum $k^3P(k)$ (measure of inhomogeneities of matter distribution in the Universe at different wavenumbers $k$) for different parameters of sterile neutrino Dark Matter. The monotonically growing solid line corresponds to sterile neutrinos with negligible initial velocity dispersion (Cold Dark Matter), the other solid line – to resonantly produced sterile neutrino with mass $M_s = 7\,\mathrm{keV}$, and initial ratio of lepton number to entropy equal to $4.4\times10^{-5}$. The dotted, dashed, and dot-dashed lines correspond to sterile neutrinos with masses $M_s = 1.5\,\mathrm{keV}, 2\,\mathrm{keV}, 3.3\,\mathrm{keV}$ respectively, which have equilibrium (Fermi) form of spectrum. In each case, the abundance of the DM is matched to the observed value.

The first Sakharov condition is satisfied in the Standard Model [76]. Although the baryon number is conserved in elementary collision processes, it is violated by the quantum phenomenon called chiral anomaly [77, 78]

$$\partial_\mu j^\mu_B = \frac{3g^2}{16\pi^2}\mathrm{Tr}\left[F_{\mu\nu}\tilde{F}^{\mu\nu}\right] \tag{1.25}$$

where $j^\mu_B$ is the 4-current of baryons (the zeroth component $j^0_B$ is the baryon density), $F_{\mu\nu}$ is the strength tensor of the $SU_L(2)$ gauge field, $\tilde{F}^{\mu\nu} = \epsilon^{\mu\nu\alpha\beta}F_{\alpha\beta}$ is the dual field, $g$ is the $SU_L(2)$ coupling constant, and the trace is taken over the $SU(2)$ indices. Similarly, the lepton current $j^\mu_L$ is not conserved due to the same chiral anomaly, such that the combination $B-L$ is preserved, while $B+L$ is *not* preserved [76]. Here $B = \int d^3x j^0_B$ is the baryon number and $L = \int d^3x j^0_L$ is the lepton number. In order to use the chiral anomaly for generation of $B$, one has to generate first $L$. Here we want to note that the baryon number violation is better constrained experimentally, than the violation of lepton number [15]. The source

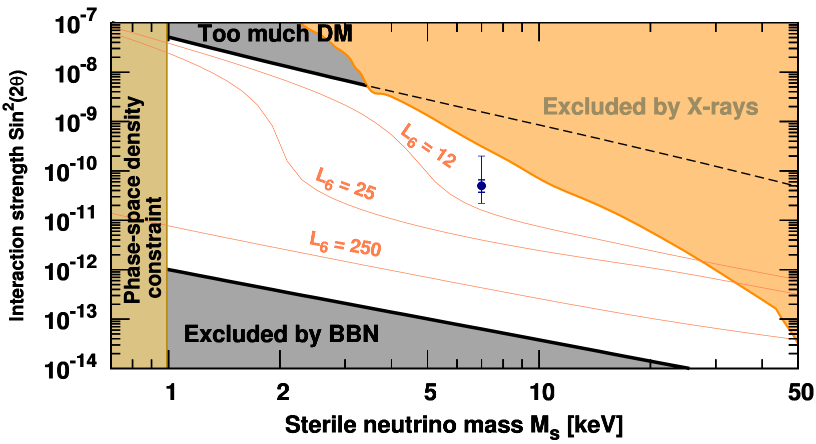


Figure 1.9: Observational constraints on the mixing angle $\theta$ of the Dark Matter sterile neutrino. The left shaded region is excluded by the Pauli principle applied to compact DM-dominated objects [30, 31], the upper black line corresponds to the non-resonant production, the right orange corner is excluded by the X-ray observations [63, 62], the region below the lower thick black line is excluded by the Big-Bang Nucleosynthesis [73, 74]. The curves labeled by different values of $L_6$ correspond to resonant production of the DM at different values of lepton asymmetry ($L_6 \equiv 10^6 L/9S$, where $L$ is the lepton number, $S$ is entropy). The point in the center with error bars corresponds to the observed 3.5keV X-ray signal [67, 68].

of lepton number violation can be provided by Majorana sterile neutrinos.

The integral of the expression $\mathrm{Tr}\,[F_{\mu\nu}\tilde{F}^{\mu\nu}]$ over time and space can take only discrete values $n$, due to its non-trivial topological properties. Therefore, in order for chiral anomaly to operate and to transform lepton number into baryon number, we need $SU(2)$ field configurations with non-zero $n$. These configurations exist and are known as sphalerons [79]. They are populated in plasma only at high temperatures, where the electroweak symmetry is unbroken ($T \gtrsim 100$ GeV).

Sterile neutrinos lead to successful leptogenesis. If they are much heavier than 100 GeV, according to the see-saw formula (1.7), they have relatively large mixing angles, so that they enter equilibrium at $T \gg 100$ GeV. While the Universe cools down, their interaction rate decreases, they fall out of thermal equilibrium ("freeze-out"), and start to decay (the third Sakharov condition). Due to CP-violation, which is present in sterile neutrino sector (the second Sakharov condition), sterile neutrinos interact a bit differently with particles and anti-particles, so that in the decays, the number of lepton and anti-leptons is different, and non-zero lepton number is generated. This is the standard scenario of thermal leptogenesis [80].

It turns out that leptogenesis works for lighter sterile neutrinos, $M_s \ll 100\text{GeV}$ as well [81, 82]. In this case, however, sterile neutrinos should not come into thermal equilibrium while the electroweak symmetry is unbroken, as we argue below. Instead, they are produced gradually in reactions of the SM particles while the Universe cools down, and due to the CP violation, in reactions with SM particles sterile neutrinos produce different amount of leptons and anti-leptons, so *non-vanishing* lepton numbers are generated. For $M_s \ll 100$ GeV, sterile neutrinos are relativistic, and for relativistic particles, mass does play much role (in particular, whether it is Dirac of Majorana). It means, that the total lepton number is effectively conserved, if one includes into this number the "sterile" lepton number. (The sterile lepton number can be defined as the difference between left-helical sterile neutrinos (particles) and the number of right-helical sterile neutrinos (antiparticles).) This way, the lepton number is *not produced* (as it happened for heavy sterile neutrinos above), but *is distributed* between active and sterile neutrinos. In thermal equilibrium, processes that increase asymmetry in active flavours go with the same speed as the processes that decrease the asymmetry, and the lepton asymmetry is washed out. Therefore, sterile neutrinos should not come into thermal equilibrium during the baryogenesis epoch (third Sakharov condition).

How the lepton numbers in different active flavours are related to each other, depends on the particular pattern of active-sterile mixing. For example, if sterile neutrinos do not couple to electronic flavour, then no asymmetry between electron neutrinos and antineutrinos is produced at high temperatures.

For successful leptogenesis, we need at least two sterile neutrinos. Note that this is the same number, as required for neutrino oscillations. And in what follows, we will implicitly assume that the sterile neutrinos which generate lepton asymmetry, explain neutrino oscillations at the same time. In order to produce the required baryon asymmetry (1.2) with two neutrinos, the CP-violating effect should be enhanced by resonance between the two neutrinos. It requires very small splitting in their masses [82].

An important feature of sphaleron transitions is that they tend to make $B \sim L$ [76]. Therefore at high temperatures, when sphalerons still operate effectively, the small value of baryon asymmetry (1.2) is accompanied by the same small value of lepton asymmetry. However, when temperature decreases below 100 GeV, and baryon number becomes conserved, the generation of lepton asymmetry still takes place, and there is no reason why the value of this asymmetry cannot exceed the value of baryon asymmetry. Production of lepton number, which is much larger than the baryon number, is the specific feature of leptogenesis with relatively light sterile neutrinos (masses below 100 GeV). Leptogenesis takes place until the sterile neutrinos finally reach thermal equilibrium ($T = T_+$). At this moment, lepton asymmetry gets washed away, according to what was said above. Sterile neutrinos spend some time in this equilibrium regime, until their collisions become so rare that thermal equilibrium ceases to hold for them. ("Freeze-out" happens, $T = T_-$.) The subsequent evolution is similar to what happens with very heavy

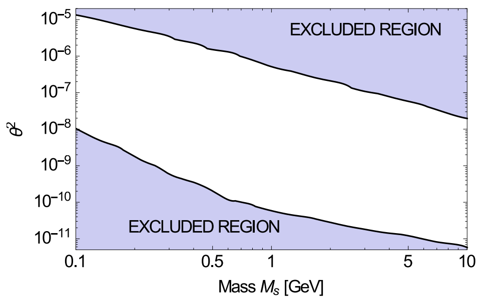


Figure 1.10: Parameter space of two sterile neutrinos which produce the observed Baryon Asymmetry of the Universe [84, 85]. The horizontal axis corresponds to the average mass of sterile neutrinos $M_s$ (the difference between the two masses is much smaller than $M_s$), the vertical axis corresponds to the average square of the mixing angle, $\theta^2$. The upper filled region is excluded, since for larger mixing angles sterile neutrinos come into thermal equilibrium before the end of baryogenesis and therefore wash out the baryon asymmetry. The lower filled region is excluded, since for smaller mixing angles, sterile neutrinos couple to plasma too weakly, and are not able to produce enough baryon asymmetry.

singlet neutrinos $M_s \gg 100$ GeV: sterile neutrinos freely propagate in plasma, until they start to decay, the numbers of particles and antiparticles produced in these decays are a bit different, so lepton asymmetry is generated again. The successful baryogenesis implies both the lower and the upper bounds on sterile neutrino mass, MeV $\lesssim M_s \lesssim 20$ GeV [81, 82, 83].

The observed value of baryon asymmetry can be generated by sterile neutrinos $N_2$ and $N_3$ with masses $M_{2,3}$ in the MeV-GeV range, provided that they have small mass splitting,

$$|M_2 - M_3| \ll M_2 \tag{1.26}$$

The generation of lepton asymmetry by these particles continues at temperatures below 100GeV, when the baryon asymmetry is no longer generated. This way lepton asymmetry can become much larger than the baryon asymmetry. If $N_1$ does not describe the Dark Matter, this particle can significantly contribute to neutrino oscillations via the see-saw mechanism, and can influence the baryogenesis. In this case, successful baryogenesis does not require smallness of the mass splitting [86], and the lightest active neutrino mass eigenstate does not have to be massless.

### 1.3.4 The Neutrino Minimal Standard Model

Since the mixing angle of the DM sterile neutrino $N_1$ is small, it does not contribute significantly to the neutrino masses via the see-saw mechanism. Therefore, in order to explain neutrino oscillations,we need at least another two sterile neutrinos, $N_2$ and $N_3$, which can simultaneously give rise to the observed baryon asymmetry. **The resulting number of right-handed neutrinos is three.** If we choose masses of sterile neutrinos below 100GeV, we get the model which is called **the Neutrino Minimal Standard model ($\nu$MSM )** [50, 82] (for a recent review, see [62]). In this model, the lightest active neutrino mass eigenstate is massless.

Although we have experimental constraints on different corners of parameter space of the $\nu$MSM, there still exists large open window. Here we want to note, that apart from the three Majorana masses $M_1, M_2, M_3$, there are 15 physically observable parameters in the Yukawa matrix $F_{\alpha I}$. In total, the model is characterized by 18 parameters [50].

If we add to the $\nu$MSM non-minimal coupling of the Higgs field to gravity, we can provide an inflationary model, which explains very well the cosmological observations [87, 88]. This way, the history of the Universe can be described up to the very early stages (Planck scales).

Having this consistent theoretical framework, we can no longer consider different phenomena independently. For example, one cannot just say that the lepton asymmetry neeeded for resonant production of Dark-Matter particles, is some given external quantity. As we have noticed above, the value of the lepton asymmetry is controlled by the properties of $N_2$ and $N_3$, so one has to consider the interplay between the properties of the light and heavy singlets consistently [85, 84].

If the large lepton asymmetry, which is needed for the resonant production of DM particles, is generated after the freeze-out of $N_{2,3}$ ($T < T_-$), we need such a small value of the mass splitting $|M_2 - M_3|$, that it becomes sensitive to radiative (loop) corrections. In order to get this small number, a fine-tuning of the $\nu$MSM parameters should be done, which makes the model “unnatural” [89]. On the other hand, if the lepton asymmetry is produced at higher temperatures ($T > T_+$), then according to the discussion in Sec. 1.3.3, singlet neutrinos come to equilibrium, and the lepton asymmetry is expected to be washed out.

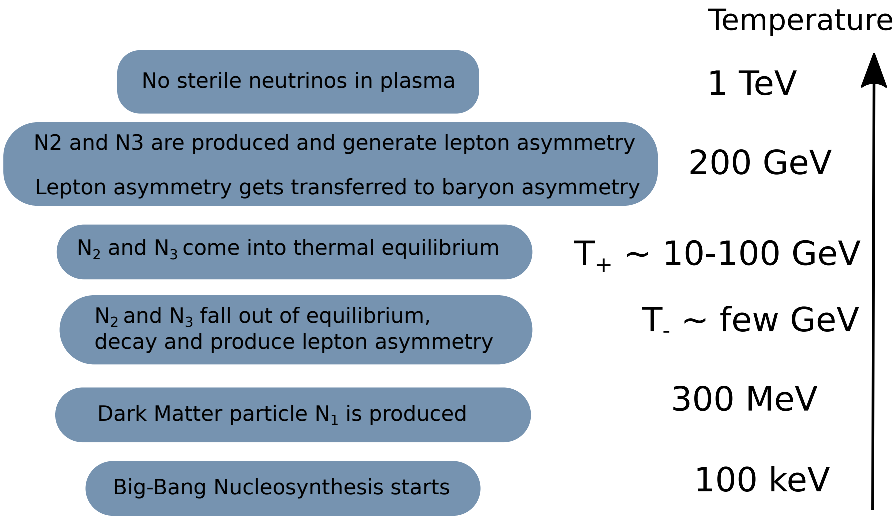


Figure 1.11: The timeline of the processes in the early Universe in the $\nu$MSM model.

The $\nu$MSM is a testable model, which is constrained by a set of independent cosmological and astrophysical observations, however the window of parameters of this model still remains open. The systematic account of the observational constraints, which is not finished at the present moment, will reduce the parameter space. For example, in order to satisfy the constraints on the DM, $N_{2,3}$ should not only produce the observed baryon asymmetry, but to produce lepton asymmetry, which is much larger than this asymmetry.
It is problematic to produce lepton asymmetry after sterile neutrinos have frozen out ($T < T_-$), while it is much easier to produce the asymmetry at higher temperatures, where sterile neutrinos are still out of thermal equilirium ($T > T_+$). However, in the intermediate region, $T_- < T < T_+$, sterile neutrinos come into thermal equilibrium, and how does the lepton asymmetry evolve here is an open question. Below, we consider an *additional* effect, which is important for the description of lepton asymmetry at these intermediate temperatures.

The timeline of the processes in the early Universe in the $\nu$MSM model is plotted in Fig. 1.11.

### 1.3.5 Lepton asymmetry and magnetic fields

Due to the parity-violating nature of the interactions of SM fermions with electroweak gauge bosons ($W$, $Z$ and photons), interactions of sterile neutrinos with left and right SM charged fermions are different. Therefore, left and right particles are produced in different amounts during the leptogenesis. Namely, only neutrinos interact with sterile neutrinos. Fast interactions with $W^{\pm}$ bosons equilibrate the number density of neutrinos and charged leptons (electrons, muon, tau leptons). However, all the gauge interactions respect chirality, and therefore do not change the asymmetries in sectors of left and right particles. Nevertheless, a disbalance between these two sectors gets relaxed to zero since all the charged particles are massive, therefore the numbers of left and right particles are not conserved individually. Namely, there exist collision processes (*chirality-flipping processes*), in which left particle can transform into right one. An example of such a process is Compton scattering, $e_{\rm L}\gamma \to e_{\rm R}\gamma$, where $e_{\rm L}$ and $e_{\rm R}$ are left and right electrons, respectively, and $\gamma$ is a photon. However, these chirality-flipping processes are relatively slow, chirality-flipping rate $\Gamma_{\rm flip}$ is suppressed with respect to the rate of ordinary collisions (*chirality-preserving rate*) $\Gamma_{\rm LTE}$ as $m^2/T^2$, where $m$ is the fermion mass. Therefore, two different timescales appear in the problem.[4]

The first timescale, $\sim \Gamma_{\rm LTE}^{-1}$, corresponds to the time when partial equilibrium is established in the left and right sector of the theory *separately*, bringing the momentum distribution in each of the sectors to the Fermi-Dirac form:

$$f_{\rm L}(\boldsymbol{p}) = \frac{1}{\exp\left(\frac{E_{\boldsymbol{p}}-\mu_{\rm L}}{T}\right)+1}, \quad f_{\rm R}(\boldsymbol{p}) = \frac{1}{\exp\left(\frac{E_{\boldsymbol{p}}-\mu_{\rm R}}{T}\right)+1}, \tag{1.27}$$

where the chemical potentials $\mu_{\rm L}$ and $\mu_R$ of these distributions are *independent*, so that the axial chemical potential is non-vanishing,

$$\mu_5 \equiv \mu_{\rm L} - \mu_{\rm R} \neq 0 \tag{1.28}$$

The second timescale, $\Gamma_{\rm flip}^{-1} \gg \Gamma_{\rm LTE}^{-1}$, is much longer than the first one, and corresponds to the time when particles reach equilibrium *between* left and right sectors, due to their mass term and due to the residual Higgs boson decays, $H \to e_{\rm L} + \bar{e}_{\rm R}$, so that at these times *left and right particles are described by the Fermi-Dirac distribution with a common chemical potential*, $\mu = (\mu_{\rm L} + \mu_{\rm R})/2$, corresponding to the conserved fermion number.

In other words, fermions spend some time with chiral asymmetry, while having equilibrium spectra (1.27). The chiral imbalance in the plasma of charged particles has drastic consequences for its evolution.

### 1.3.6 Electric current along the magnetic field

In order to demonstrate how does the chiral imbalance affect the system of charged particles, we will use the quantum mechanical description, originally presented in the pioneering work [90]. Namely, we consider the system of charged fermions (massless for simplicity) in the uniform magnetic field, pointing along the $z$ axis.

[4] This is of course a simplification. Below we discuss the simplest case when only electrons, neutrinos and sterile neutrinos are present in the plasma, to avoid discussing the whole hierarchy of times, related to different particles, leptons vs. quarks, etc.

Particles occupy the so-called Landau levels. The energies of these levels are characterized by one discrete integer number $n \geq 0$ and *one* continuous number – momentum $p_z$ along the direction of the field,

$$\varepsilon_n(p_z) = \sqrt{p_z^2 + 2|eB|n}, \qquad n = 0, 1, 2\ldots \tag{1.29}$$

The level with $n = 0$ (*lowest Landau level*) is different from $n > 0$ levels. The motion of particles is that of *free one-dimensional massless fermions* with $\varepsilon_0(p_z) = \pm|p_z|$ with *their spin always pointing opposite to the direction of the magnetic field*. Therefore the particles with $p_z > 0$ have negative projection of spin onto momentum (so called *left-chiral* particles) and the particles with $p_z < 0$ have positive projection of the spin onto momentum (right-chiral particles).[5] The allowed range of $p_z$ is different for $n = 0$ and $n > 0$, namely

$$-\infty < p_z < \infty \quad (n \neq 0, \quad \text{both chiralities}) \tag{1.30}$$

$$0 \leq p_z < \infty \quad (n = 0, \quad \text{left chirality}) \tag{1.31}$$

$$-\infty \leq p_z \leq 0 \quad (n = 0, \quad \text{right chirality}). \tag{1.32}$$

(these ranges hold for both particles and anti-particles.)

In the vacuum (at zero temperature and zero chemical potentials) all the states with $\varepsilon_n(p_z) < 0$ are filled (the *Dirac sea*) while all the states with $\varepsilon_n(p_z) > 0$ are empty. In thermal equilibrium, the distribution functions are characterized by chiral Fermi distributions (1.27) with $E_{\boldsymbol{p}} = \varepsilon_n(p_z)$, different for left and right particles.

Given the distribution functions, the electric current density can be calculated by the statistical formula

$$\boldsymbol{j} = e\frac{|e\boldsymbol{B}|}{2\pi}\left[\int_0^\infty \frac{dp^z}{2\pi}\,\psi_{p^z}\boldsymbol{\gamma}\psi_{p^z} f_{\mathrm{L}}(p^z) + \int_{-\infty}^0 \frac{dp^z}{2\pi}\,\bar{\psi}_{p^z}\boldsymbol{\gamma}\psi_{p^z} f_{\mathrm{R}}(p^z)\right] + \text{anti-particles}+ \\ + \text{sum over Landau levels with } n > 0 \tag{1.33}$$

(where $\psi_{p^z}$ are the eigen functions of the Dirac equation on the lowest Landau level, and the factor $|eB|/2\pi$ is the number of states with given momentum $p^z$, per two-dimensional area perpendicular to the direction of the magnetic field). The sum over the higher Landau levels does not contribute to the current and therefore only the first line in (1.33) gives non-zero contribution:[6]

[5] Here, for definiteness, we have chosen $eB < 0$, and this choice will be used in what follows. If the sign of $eB$ is opposite, then the directions of propagation along $z$ are flipped: the left-chiral states have then $p_z < 0$, the right-chiral states have $p_z > 0$.

[6] We use **bold** notations for 3-dimensional vectors, $\boldsymbol{x}$, $\boldsymbol{A}$. Their components are denoted with Latin indices $i$. 4-dimensional vectors are denoted by $p, q$ etc and Greek indices run from $0\ldots3$.

$$\boldsymbol{j} = -\frac{e^2}{4\pi^2}(\mu_{\rm L} - \mu_{\rm R})\boldsymbol{B} \tag{1.34}$$

This current, flowing along the direction of the magnetic field and proportional to the chiral imbalance, is known as *chiral magnetic current* or *chiral magnetic effect* (CME).

### 1.3.7 Chiral Magnetic Effect

In the field-theoretical approach, the existence of the Chiral Magnetic Current (1.34) signals a presence of the *parity-odd part* of the low-energy effective action (free energy) of the gauge fields,

$$\mathcal{F}[\boldsymbol{A}] = \frac{1}{2}\int d^3\boldsymbol{q}\, A^i(-\boldsymbol{q})\Pi^{ij}(\boldsymbol{q})A^j(\boldsymbol{q}) \tag{1.35}$$

where the parity-odd part of the polarization operator $\Pi^{ij}$ is fixed by the gauge and rotational invariance to be of the form

$$\Pi_2^{ij}(\boldsymbol{q}) = -i\epsilon^{ijk}q^k\Pi_2(\boldsymbol{q}^2) \tag{1.36}$$

If $\Pi_2(0) \equiv \Pi_{\rm CS} \neq 0$, then a parity-odd *Chern-Simons term*,

$$\mathcal{F}_{\rm CS}[\boldsymbol{A}] = \Pi_{\rm CS}\int d^3\boldsymbol{x}\, \boldsymbol{A}\cdot\boldsymbol{B}, \tag{1.37}$$

is a part of the free energy (1.35). The current due to the field $\boldsymbol{A}(\boldsymbol{q})$ is given of course as

$$\langle j^i(\boldsymbol{q})\rangle = \frac{\delta\mathcal{F}[\boldsymbol{A}]}{\delta\boldsymbol{A}} = \Pi^{ij}A^j(\boldsymbol{q}) \tag{1.38}$$

The non-zero $\Pi_{\rm CS}$ leads to the current

$$\boldsymbol{j} = \Pi_{\rm CS}\nabla\times\boldsymbol{A} \tag{1.39}$$

which is just the current (1.34) after the identification

$$\Pi_{\rm CS} = -\frac{e^2}{4\pi^2}(\mu_{\rm L} - \mu_{\rm R}) \tag{1.40}$$

The Chern-Simons term has less derivatives than the usual kinetic term $\int d^3x\frac{\boldsymbol{B}^2}{2} = -\int d^3q\frac{(\boldsymbol{q}\times\boldsymbol{A})^2}{2}$ and is therefore more relevant for the infrared physics (i.e., when the wavenumbers $\boldsymbol{q}$ are very small). However, the Chern-Simons term (1.37) is no positive definite, since it involves the odd (first) power of derivative. As a result, the effective action for the electromagnetic fields in the medium with chiral imbalance is unbounded from below for sufficiently small $|\boldsymbol{q}|$ and we can expect the development of instability for $\boldsymbol{A}(\boldsymbol{q})$. And indeed, the Maxwell equations with the current (1.34) are unstable against generation of gauge fields with $|\boldsymbol{q}| \ll \Pi_{\rm CS}$ [91, 92, 93, 94].

### 1.3.8 Chiral anomaly and dynamics of chiral imbalance

Not only the presence of chiral imbalance changes the dynamics of electromagnetic fields, but also the electromagnetic fields themselves affect the change in time of the chiral chemical potential. This coupling is the consequence of the phenomenon, called quantum anomaly, which was mentioned in context of baryon asymmetry and sphaleron transitions in Sec. 1.3.3. The phenomenon of chiral (or axial) anomaly was known for many decades [77, 78], which is basically the non-conservation of axial fermionic charge $j^{\mu 5} = \langle \bar{\psi}\gamma^\mu\gamma^5\psi \rangle$ in presence of strong electric $\boldsymbol{E}$ and magnetic $\boldsymbol{B}$ fields,

$$\partial_\mu j^{\mu 5} = -\partial_\mu j^\mu_{\rm L} + \partial_\mu j^\mu_{\rm R} = \frac{e^2}{2\pi^2}\boldsymbol{E}\cdot\boldsymbol{B}. \tag{1.41}$$

Here $j^\mu_{\rm L}$ is the electric current density of left-chiral particles, $j^\mu_{\rm R}$ is the contribution of their right-chiral counterparts. Since the magnetic field is unstable, it becomes time-dependent, which induces the electric field, according to the Faraday law, $\boldsymbol{\nabla}\times\boldsymbol{E} = -\partial_0\boldsymbol{B}$. In presence of both electric and magnetic fields, the chiral anomaly starts to operate. Although separately the left- and right-chiral charges are not conserved, their sum is conserved,

$$\partial_\mu(j^\mu_{\rm L} + j^\mu_{\rm R}) = 0. \tag{1.42}$$

This latter requirement is crucial for self-consistency of the theory, otherwise the gauge invariance of the theory is lost. (At the same time, we do not associate the axial current $j^{\mu 5}$ with any kind of gauge symmetry, so the non-conservation of this latter current does not spoil the theory).

As a result of chiral anomaly, the left and right charges get changed, while the combinations

$$\tilde{Q}_{\rm L} = \int d^3x \left( j^0_{\rm L} - \frac{e^2}{4\pi^2}\boldsymbol{A}\boldsymbol{B} \right) \tag{1.43}$$

$$\tilde{Q}_{\rm R} = \int d^3x \left( j^0_{\rm R} + \frac{e^2}{4\pi^2}\boldsymbol{A}\boldsymbol{B} \right) \tag{1.44}$$

are preserved with time. Therefore, it is natural to call these two combinations as generalized chiral charges. One may check, that at zero temperature, the conservation of the generalized charges leads to a *reduction* of the energy splitting $\mu_{\rm L} - \mu_{\rm R}$ between the two Fermi levels $\varepsilon_p = \mu_{\rm L}$ and $\varepsilon_p = \mu_{\rm R}$, with time, provided that the Chern-Simons contribution to the energy density (1.37) is negative. In other words, magnetic fields get produced by "absorbing" the fermionic disbalance, and in the asymptotic equilibrium state, one expects that the Fermi levels for different chiralities become indistinguishable.

Inclusion of temperature does not change qualitatively the picture above, since the form of the electric current (1.34) is independent of the temperature, and is applicable at all temperatures. The system of hydrodynamic equations is

$$\boldsymbol{\nabla E} = \rho, \quad \boldsymbol{\nabla B} = 0, \tag{1.45}$$

$$\boldsymbol{\nabla} \times \boldsymbol{E} = -\frac{\partial \boldsymbol{B}}{\partial t}, \quad \boldsymbol{\nabla} \times \boldsymbol{B} = -\frac{e^2}{4\pi^2}(\mu_{\mathrm{L}} - \mu_{\mathrm{R}})\boldsymbol{B} + \sigma \boldsymbol{E} + \frac{\partial \boldsymbol{E}}{\partial t}, \tag{1.46}$$

$$\frac{\partial(\mu_{\mathrm{L}} - \mu_{\mathrm{R}})}{\partial t} = -\frac{3e^2}{\pi T^2}\boldsymbol{E} \cdot \boldsymbol{B} - \Gamma_{\mathrm{flip}}(\mu_{\mathrm{L}} - \mu_{\mathrm{R}}). \tag{1.47}$$

which are the Maxwell equations together with the Adler-Bell-Jackiw equation (1.41), where in the last one, the axial current is rewritten through chemical potentials. Note the inclusion of the Ohmic current $\sigma \boldsymbol{E}$, where $\sigma$ is the conductivity of plasma. In what follows, we consider an electrically neutral plasma, so that the charge density $\rho$ vanishes, $\rho = 0$. Another important simplification is that we consider relatively slow evolution of the system, so that the displacement current $\partial \boldsymbol{E}/\partial t$ can be neglected, as compared to the Ohmic current. One notes, that in the Adler-Bell-Jackiw equation, we have added contribution $-\Gamma_{\mathrm{flip}}(\mu_{\mathrm{L}} - \mu_{\mathrm{R}})$, which describes the change of chirality due to particle collisions (the abovementioned chirality-flipping processes), and this tern is not related directly to chiral anomaly. $\Gamma_f$ has the sense of the chirality-flipping rate (number of chirality-flipping reactions for a given particle, per unit time).

Going to Fourier space with respect to spatial coodinate $\boldsymbol{x}$, we find that the electric and magnetic fields are transversal, $\boldsymbol{q} \cdot \boldsymbol{E} = \boldsymbol{q} \cdot \boldsymbol{B} = 0$. Excluding the electric field, we get

$$\frac{\partial \boldsymbol{B}}{\partial t} = -\frac{1}{\sigma}(q^2 \boldsymbol{B} + i\frac{e^2}{4\pi^2}\mu_5\, \boldsymbol{q} \times \boldsymbol{B}). \tag{1.48}$$

Here the shorthand notation $\mu_5 = \mu_{\mathrm{L}} - \mu_{\mathrm{R}}$ for the chiral disbalance was introduced. The term with $\mu_5$ in the right-hand side involves first power of wavenumber $q$, while the other term in the right-hand side involves the second power of $q$. The wavenumbers where the term with $\mu_5$ becomes larger than the term with $q^2$, are

$$q \ll \frac{e^2}{4\pi^2}\mu_5 \tag{1.49}$$

In this infrared region, the term with $\mu_5$ dominates the dynamics of the magnetic field. On the other hand, the sign of this term depends on the helicity of the magnetic field (whether it is left- or right-helical), therefore one of the helicities grows exponentially with time [92], which is the sign of the instability, which was mentioned above.

Having in mind the setup of very early Universe, the chirality-flipping rate is known to be larger than the Hubble expansion rate

$$H \sim \frac{T^2}{M_{\rm pl}}, \tag{1.50}$$

at temperatures $T \lesssim 80$ TeV [95]. (Here $M_{\rm pl} \sim 10^{19}$ GeV is the Planck mass.) This result means, that chirality-flipping reactions are very active at these temperatures, and the anomalous instability process does not take place: instead of producing magnetic fields, the chiral disbalance is washed away by collision processes.

Therefore, we see that magnetic field affects the evolution of the chiral asymmetry $\mu_{\rm L} - \mu_{\rm R}$, and these two quantities get coupled. Considered separately, both chiral asymmetry (destroyed by chirality flips) and magnetic fields (destroyed by magnetic diffusion) would disappear from the plasma relatively fast. The picture changes, however, if their coupled evolution is considered.

It was shown recently [96, 97], that the evolution of this coupled system is non-trivial, and large chiral asymmetry together with magnetic fields that are triggered by this asymmetry may survive as long as plasma has charged fermions which are still relativistic. Recalling that the lightest charged fermion is electron, and that it has mass 0.5 MeV, magnetic fields can survive up to temperatures of few MeV.

Moreover, weak interaction violates parity symmetry and therefore the effective properties of the left and right electrons in dense medium are not the same. It was therefore argued in [98], that even if $\mu_{\rm L} = \mu_{\rm R}$ (or if the chiral asymmetry in the initial state of the system is small), in the presence of *lepton asymmetry* weak interactions can trigger Chiral Magnetic Effect. This would mean that even the equilibrium state of the SM plasma at high temperatures should be populated by magnetic fields.

Although lepton asymmetry disappears from the plasma once sterile neutrinos enter thermal equilibrium, if strong helical magnetic fields are generated as a by-product of this lepton asymmetry, there is no reason for these magnetic fields to disappear when sterile neutrinos are in thermal equilibrium. Then, once sterile neutrinos are out of equilibrium again, the same CME and chiral asymmetry that accompany helical magnetic fields would quickly regenerate effective lepton asymmetry in the plasma.

Lepton and chiral asymmetries are coupled to magnetic fields. In order to make a reliable prediction of the lepton asymmetry evolution in the temperature range $T_- < T < T_+$ in the $\nu$MSM (which is important for determination of the DM abundance), one has to understand the coupled dynamics of these degrees of freedom. The steps towards systematic exploration of this question are made in Chapters 4 and 5.

### 1.3.9 Accelerator searches of sterile neutrinos

Sterile neutrinos can be searched at particle accelerators [99]. A number of accelerator searches was carried out in the past and are planned for the future. The main strategy of these searches is not to increase the energies of the colliding particles, as it takes place in the LHC collider, where the center-of-mass energy is of order of 10TeV (*high-energy frontier*), but to reach high statistics of the rare events (*high-intensity frontier*).
Cosmological bounds play here important role, since they reduce the wide window of possible parameters of the model for such terrestial searches. The $\nu$MSM can be regarded here as a benchmark bottom-up model, which illustrates how well can we explore the parameter space using methods of particle physics, cosmology and astrophysics.
The systematic account of cosmological and accelerator constraints of the $\nu$MSM is not finished at the present moment, and the current thesis attempts to make a step in this direction.

The past experiments are reviewed in Chapter 2. Here we want to describe one of the most promising *future* experiments to search for the two heavier $\nu$MSM neutrinos, the SHiP experiment (Search for Hidden Particles) [100, 101, 102] (the website of the collaboration is http://ship.web.cern.ch/ship/). This experiment is a proposed general-purpose fixed target facility at the CERN SPS (Super Proton Synchrotron).

The setup of the SHiP experiment is plotted in Fig. 1.12. The incoming flux of protons with energy 400GeV from the SPS accelerator hits the dense fixed target. As a result of strong interactions, a flux of secondary hadrons (pions, kaons, $D$-mesons) is produced, and these unstable secondary particles decay into charged leptons and neutrinos, where in addition of active neutrinos, a small admixture of sterile neutrinos appears. The thick wall of absorbing material behind the target ensures that no charged particles pass through it. Next to the wall, the large decay volume is placed, where the decays of new unstable neutral particles can be detected. In this scheme, sterile neutrinos are produced in decays of $D$-mesons, and can be detected in different two- and three-body decay channels like $N \to \pi^+ e^-$ and $N \to \nu e^+ e^-$.

In the SHiP experiment the center-of-mass energy of the colliding particles (which are the proton from SPS and a proton of the target nucleus) is just several

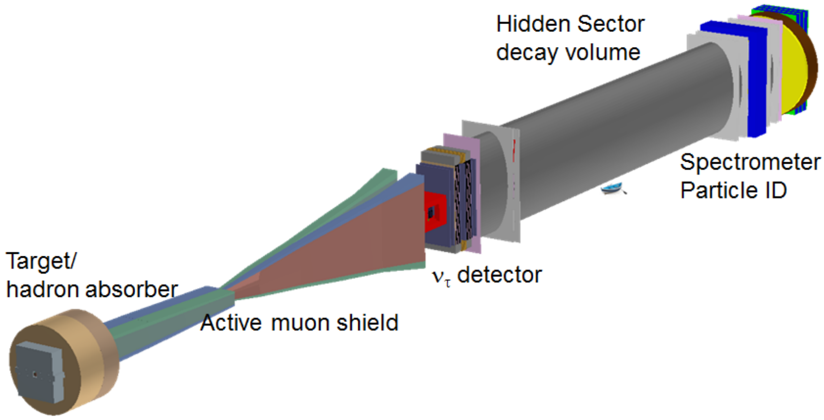


Figure 1.12: The setup of the SHiP experiment [102]. The incident proton beam from the SPS accelerator hits the target, the charged particles are stopped in the active muon shield, while the unstable neutral particles reach the decay volume, where they decay.

tenths of GeV. However, the expected number of protons, which hit the target in this experiment during the 5 years of running, is of order of $10^{20}$, which is a tremendous number. This way, the high-intensity frontier is reached.

The mass of the $D$-meson is approximately 2 GeV, therefore SHiP is not sensitive to sterile neutrinos heavier than 2 GeV. In order to probe the range of larger masses, one can study the decays of heavier mesons [86], $B$-mesons, which have mass around 5 GeV and are produced in large quantities in experiments like LHCb and Belle.

For $M_s > 5$ GeV, searches at high-energy frontier experiments become more perspective. An example of the planned experiment is FCC-ee [103], which is an electron-positron collider. At this experiment, a large amount of real $Z$ bosons are produced (up to $10^{13}$ in a few years), which can decay into sterile neutrino.

## 1.4 This thesis

### 1.4.1 Chapter 2

In Chapter 2, we study the pattern of the mixings between the Standard Model (active) neutrinos and their right-chiral (sterile) counterparts, which give rise to active neutrino masses via the see-saw mechanism. The bounds on these mixings are derived by combining neutrino oscillation data and results of direct accelerator searches. We reinterpret the results of searches for sterile neutrinos by the PS191 and CHARM experiments, considering not only charged current but also neutral current-mediated decays, as applicable in the case of the $\nu$MSM. The resulting *lower bounds* on sterile neutrino lifetime are up to an order of magnitude *stronger* than previously discussed in the literature. We demonstrate that the mixing of sterile neutrinos with any given active flavour can be significantly suppressed, as compared to the mixings with two remaining flavours.

### 1.4.2 Chapter 3

In Chapter 3, we analyze the influence of sterile neutrinos on the Big-Bang Nucleosynthesis, in particular the primordial abundances of Helium-4 and Deuterium. We solve explicitly the set of kinetic equations (Boltzmann equations) for all particle species, which are driven out of thermal equilibrium by presence of sterile neutrinos, and we take into account neutrino flavour oscillations. We demonstrate that the nuclear abundances are sensitive *mostly* to the sterile neutrino lifetime and only weakly to the way how the active-sterile mixing is distributed between flavours. The decays of sterile neutrinos also perturb the spectra of (decoupled) active neutrinos and heats photons, changing the ratio of neutrino to photon energy density, that can be interpreted as extra neutrino species at later epochs. We derive upper bounds on the lifetime of sterile neutrinos based on both astrophysical and cosmological measurements of Helium-4 and Deuterium. Combination of these results with the lower bound on the lifetime from Chapter 2 rules out the possibility that two sterile neutrinos with the masses between 10 MeV and the pion mass are solely responsible for neutrino flavour oscillations.

### 1.4.3 Chapter 4

In the Chapter 4, we are interested in the dynamics of primordial plasma after the baryogenesis and long before the primordial nucleosynthesis. As we have argued before, the leptogenesis in the $\nu$MSM still takes place at these intermediate temperatures, and the chiral asymmetry is produced as a by-product. Therefore, the Chiral Magnetic Effect may become important, and trigger the growth of magnetic fields. The scale of coherence of the magnetic fields, however, is very large. On the other hand, we know that charged particles, which are the key ingridient for the Chiral Magnetic Effect, are massive, and their mass $m$ is larger than the inverse lengthscale, $q$, of the magnetic field. However, in the literature the fermion mass is usually neglected, which corresponds to the opposite limit, $q \gg m$. As a result, the calculation of the current is made for massless fermions, two different chiralities of which are in thermal equilibrium with its own chemical potential, either $\mu_\mathrm{L}$ or $\mu_\mathrm{R}$ (Note that we have considered this approximation in the actual derivation of the Eq. (1.34).) However, strictly speaking, massive fermions do not have a definite chirality anymore, and are not in the state of thermal equilibrium, due to chirality-flipping processes, so the calculation of the current is not straightforward. In order to overcome this difficulty, we consider two systems. In the first one, we consider a definite ensemble of quantum-mechanical states, which corresponds to the (local) thermal equilibrium on the one hand, and is characterized by chiral asymmetry, on the other hand. In the second system, the chiral asymmetry is introduced at the level of the particle dispersion relation, by introducing axial self-energy of the form (4.21). Therefore, the asymmetry is expected to be present in the state of thermal equilibrium, which allows application of the standard equilibrium method of imaginary-time field theory (Matsubara technique). However, if one proceeds in a straightforward way, we argue that one does not necessarily get the correct answer for the electric current.

### 1.4.4 Chapter 5

As we have mentioned above, the analysis [98] indicates that the Chern-Simons term *is* induced by parity-violating particle interactions in a theory with local four-fermion interaction (Fermi theory). However, we know that in the Standard Model, this interaction is actually non-local, but is mediated by massive $W$- and $Z$-bosons. Therefore, in Chapter 5 we extend the original study [98] to a simplified theory with *one* massive boson, which mediates the parity-violating four-fermion interaction. The conclusion is that different contributions to the Chern-Simons term in plasma cancel each other, so that no parity-odd effective action is induced for the electromagnetic field. We argue that the reason of this apparent conflict with the result of the local theory lies in that the prediction for the Chern-Simons term in Fermi theory actually involves an ambiguity, which was not taken into account before.